Performance of helical piles in oil sand

Mohammed Sakr

Abstract: The results of a comprehensive pile load-test program and observations from field monitoring of helical piles with either a single helix or double helixes installed in oil sand are presented in this paper. Eleven full-scale pile load tests were carried out including axial compression, uplift, and lateral load tests. The results of the full-scale load tests are used to develop a theoretical design model for helical piles installed in oil sand. Test results confirm that the helical pile is a viable deep foundation option for support of heavily loaded structures. The test results also demonstrated that circular-shaft helical piles can resist considerable lateral loads.

Key words: helical piles, screw piles, oil sands, full-scale load tests, compression, uplift, lateral.

Résumé : Cet article présente les résultats d'un programme d'essais de chargement de pieux, et d'un programme de suivi de pieux hélicoïdaux avec soit une ou deux hélices installés dans les sables bitumineux. Onze essais de chargement de pieux à l'échelle réelle ont été effectués incluant des essais de compression axiale, de soulèvement et de chargement latéral. Les résultats des essais à l'échelle réelle sont utilisés pour développer un modèle de conception théorique pour des pieux hélicoïdaux installés dans des sables bitumineux. Les résultats des essais confirment qu'un pieu hélicoïdal est une option valable pour des fondations profondes qui supportent des structures lourdement chargées. Les résultats des essais ont aussi démontré que les pieux hélicoïdaux à arbre circulaire peuvent résister à des charges latérales considérables.

Mots-clés : pieux hélicoïdaux, pieux vissés, sables bitumineux, essais de chargement à l'échelle réelle, compression, soulèvement, latéral.

[Traduit par la Rédaction]

Introduction

A helical pile (or screw pile) consists of a central shaft that is made from round or square sections with one or more formed steel plates (helixes) welded to the shaft. A shaft diameter varies between 73 and 965 mm, while helix diameter varies between 152 and 1219 mm. A single helix or multiple helixes may be used depending on the soil conditions and the required pile capacities. Helical piles can be designed to resist a variety of axial loads ranging from 50 to 5000 kN. Moreover, helical piles can be used in groups to support larger axial loads and piles with inclinations up to 45° to resist large lateral loads.

Helical piles are used extensively in western Canada and the USA to support residential buildings, commercial buildings, and industrial facilities. The use of helical piles for foundations offer many advantages including their high compressive and uplift capacities (three to five times that of traditional driven steel piles with the same shaft diameter and length[1]) rapid speed of their installation (10 m of helical pile can be typically installed in about 3 min), suitability for construction in very limited access conditions, ease of installation in frozen or swampy soil conditions, and cost effectiveness. Moreover, an unlimited pile length can be installed in the field to target the competent soil layer through the addition of extension segments. In addition, helical pile installation is a vibration-free process. Therefore, the installation of helical piles in urban areas is very favourable in terms of low level of noise and minimal vibration to nearby structures.

Received 29 May 2008. Accepted 30 March 2009. Published on the NRC Research Press Web site at cgj.nrc.ca on 27 August 2009.

M. Sakr. Almita Manufacturing Ltd., 6606 – 42nd Avenue, Ponoka, AB T4J 1J8, Canada (e-mail: mohammed@almita.com).

[1]Sakr, M., Mitchells, R., and Kenzie, J. Pile load testing of helical piles and driven steel piles in Anchorage, Alaska. Submitted to the Deep Foundations Institute (DFI) 34th Annual Conference On Deep Foundations, Kansas City, Miss., 21 – 23 October 2009.

The axial capacity of helical piles may be estimated analytically using either the individual bearing or cylindrical shear methods. The individual bearing method (Meyerhof and Adams 1968; Vesic 1971; Canadian Geotechnical Society 2006) assumes that bearing failure occurs at each individual helix (Fig. 1*a*). The total axial pile resistance in compression or tension is the sum of the capacities of the individual helixes plus shaft resistance.

The cylindrical shear method (Vesic 1971; Mitsch and Clemence 1985; Das 1990; Zhang 1999) assumes that a cylindrical shear failure surface, connecting the uppermost and lowermost helixes, is formed as shown in Fig. 1*b*. The axial capacity is derived mainly from the shear resistance along the cylindrical surface and bearing resistance above the top helix for uplift loading and from the bearing resistance below the bottom helix for compression loading. The adhesion developed along the steel shaft is considered in cases where sufficient installation depth (deep pile) is provided.

The development of individual bearing or cylindrical shear failure mechanisms depends mainly on the soil type and spacing ratio. Spacing ratio (S/D) is defined as the spacing, S, between any two adjacent helical plates divided by their average diameter, D. Hoyt and Clemence (1989) and Narasimha Rao et al. (1991) indicated that for helical piles with $S/D > 1.5$ installed in cohesionless soils, the individual plate bearing method agreed better with the results of pile loading tests.

Fig. 1. Analytical models for estimating helical pile uplift capacity: (*a*) individual helix method and (*b*) cylindrical shear method.

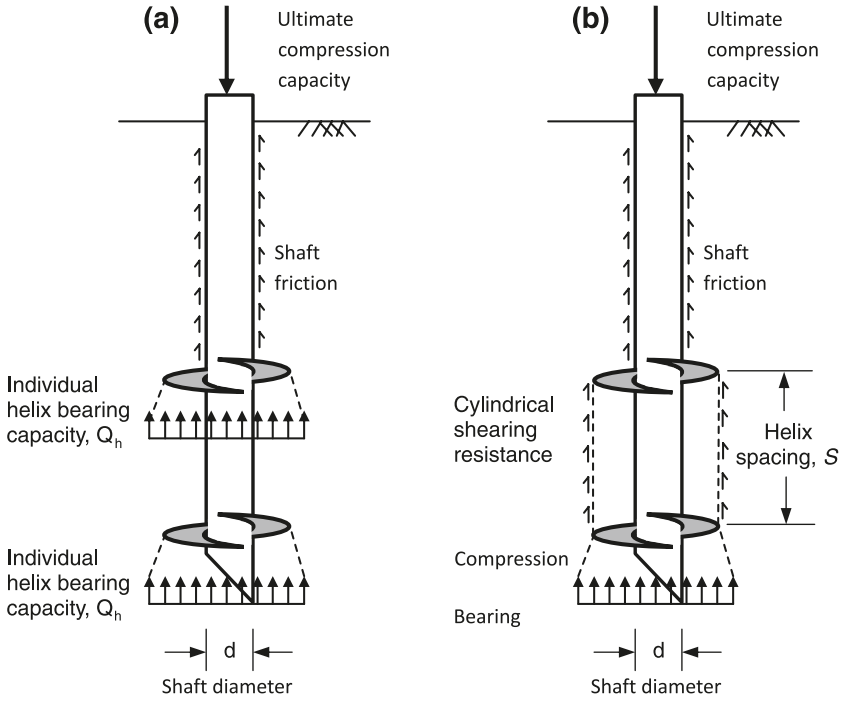

Several numerical analyses have been carried out to investigate the axial behaviour of helical piles (or circular anchors), such as Tagaya et al. (1983, 1988), Sakai and Tanaka (1998), Merifield et al. (2006), and Livneh and El Nagger (2008). Tagaya et al. (1983, 1988) carried out two-dimensional finite element analysis assuming plane strain and axisymmetric conditions for rectangular and circular anchors and using the constitutive law of Lade and Duncan (1975). Scale effects for shallow circular anchors in dense sand were estimated by Sakai and Tanaka (1998) using a constitutive model of non-associated strain-hardening–softening elasto-plastic materials. Merifield et al. (2006) investigated the effect of the anchor shape on the uplift capacity of circular and rectangular anchors using a three-dimensional finite element formulation. They concluded that the circular shape of anchors provide higher uplift resistance compared with the square anchor. Livneh and El Nagger (2008) have investigated the load transfer mechanism of square-shaft, small-diameter, multi-helical piles using a three-dimensional finite element. They concluded that the load transfer mechanism was through the cylindrical shear failure surface.

The rapid growth in Alberta motivated by the multi-billion dollar oil sand development projects in northern Alberta has necessitated construction of a variety of medium to heavily loaded structures supported on deep foundations. Due to the presence of oil sand at relatively shallow depths, piles supporting these structures are typically seated in oil sand. Helical piles used to date support residential camps, office buildings, pumps, machine foundations, pipe racks, oil tanks, and tie backs.

The main objective of the present study is to evaluate the axial and lateral performance of helical piles based on the results of full-scale loading tests. The specific objectives of the test program were to: (*i*) define appropriate failure criteria for helical piles installed in oil sand, (*ii*) evaluate their axial compressive and tensile capacities, (*iii*) correlate between installation torque and the capacity of piles, and (*iv*) investigate the performance of helical piles under lateral loads. To achieve these objectives, 11 full-scale load tests were carried out. The testing program included four axial compressive tests, five axial tensile (uplift) tests, and two lateral tests. Details of the testing program are described in the next sections.

Test pile configurations

Two pile configurations were considered for the study including single and double helix piles as illustrated in Fig. 2. The test piles were manufactured by Almita Manufacturing Ltd. of Ponoka, Alberta. Each pile was composed of a central cylindrical shaft with a diameter of 177.8 mm, 5.8 m long, with single or double helixes of 406 mm diameter and 19.1 mm thick. Double helix piles were fabricated such that the spacing ratio (*S*/*D*) equaled 3 to reduce the interaction of the bearing resistances between helixes. The pitch for each helix was 150 mm and the helical shape of the bearing plates facilitated pile installation.

Site investigation

The test location was Cree Burn Lodge located north of Fort McMurray, Alberta, just west of Highway 63 at the Albian Sand Junction and east of the Athabasca River. The site had been cleared and was originally covered with thick forest and brush. The topography of the site is relatively flat and was graded in the summer of 2007.

The test program consisted of 11 full-scale load tests carried out in two phases at two different locations on the site. Phase 1 was carried out between 5 July 2007 and 9 July 2007 and included a total of six tests (two axial compression, two axial tension (uplift), and two lateral load tests). Phase 2 was carried out between 6 January 2008 and 12 Jan-

Fig. 2. Test pile configurations.

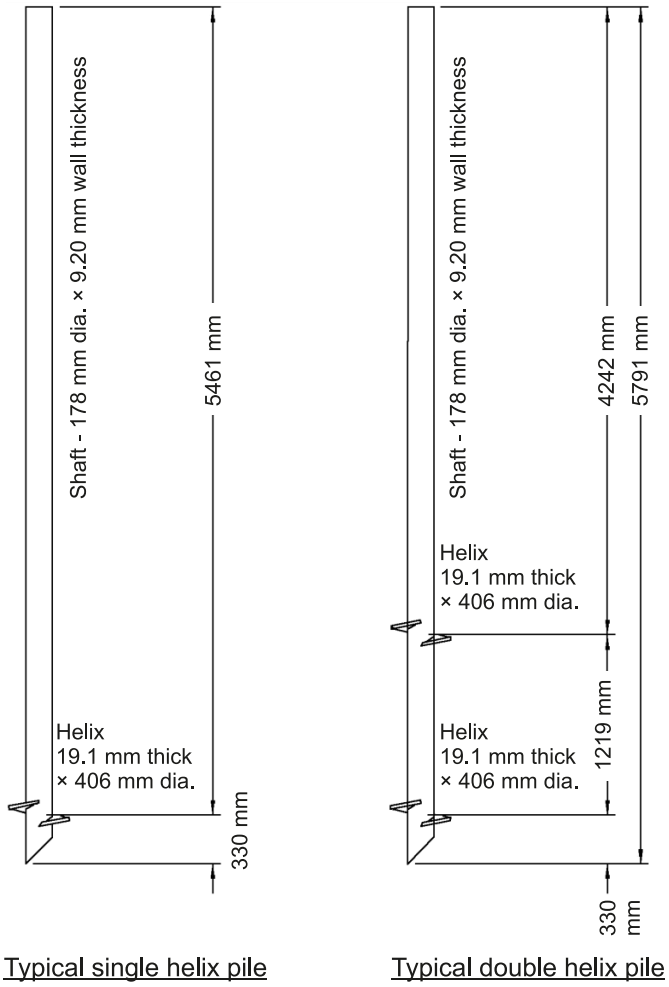

uary 2008 and included five tests (two compression and three uplift tests). Table 1 summarizes the testing schedule, pile configuration, and installation results. Phase 1 was carried out in a location near the central part of the site while phase 2 was carried out in the northwest corner of the site (due to inaccessibility of the central part at the time of testing). Phase 1 and 2 test locations were about 100 m apart.

The soils at the site consisted of fine- to medium-grained, compact to dense, moist to wet sand extending to depths ranging from 1.1 to 2 m, underlain by dense to very dense oil sand. The sand was brown, medium-grained and contained traces of gravel. The standard penetration test (SPT) indicated *N*-indices for the sand layer ranging from 11 to 22 blows per 300 mm of penetration, indicating compact sand. A summary of SPT test results for both test locations are presented in Table 2.

The oil sand was black, silty, fine- to medium-grained, and saturated, and contained traces of gravel. *N*-indices at selected depths in the oil sand ranged from 26 to over 100 blows per 300 mm of penetration, indicating a dense to very dense state. As indicated by Sharma and Joshi (1988); Alberta's oil sand deposits of the McMurray Formation are a Lower Cretaceous unit consisting of uncemented quartz sand with interbedded clay shale. The oil sand is typically composed of the following components (Scott and Kosar 1984): (*i*) fine- to medium-grained uniform quartz sand and (*ii*) pore fluids consisting of bitumen, water, and occasionally free gas. The sand grains are wet and the water forms a continuous phase throughout the oil and sand matrix. Bitumen occupies the remaining pore space. Dissolved gases are found within the liquid phases and some free gas is occasionally present depending on in situ temperatures and phases.

The groundwater level was relatively high and was measured at depths varying between 0.5 to 2 m below existing ground. Laboratory tests carried out on selected soil samples indicated that the total and dry unit weights, respectively, were about 22 and 19 kN/m^3 for the sand and 21.6 and 18 kN/m^3 for the oil sand. A summary of typical soil properties is presented in Table 3. Results of triaxial compression tests on high quality cores in undisturbed oil sand samples (Sharma et al. 1986) indicated a peak frictional angle of 50° and residual friction angle of 38°.

Pile installation and test setup

Pile installation

Helical piles are installed through the application of mechanical torque at the pile head. Torque applied at the pile head during pile installation was continuously recorded and penetration depth was measured. Final measured torque at the end of pile installation and total embedment depths are summarized in Table 1. It can be seen from Table 1 that, in general, torque values for piles tested in phase 1 were about 35% higher than torque values recorded for piles tested in phase 2. This can be attributed to the variability of oil sand depth and strength as observed from the scatter in the *N*-indices (see Table 2) and as confirmed from torque chart records. Moreover, it can be noted from Table 1 that double helix piles required, in general, about 17% to 29% higher torque values compared with single helix piles. The torque required to install pile T4 with double helixes was about 95% of that required for T3 with a single helix, which indicates localized softer soil conditions at the location of test pile T4.

Axial load test setup

The Pile load test setup consisted of either two reaction piles (phase 1) or four reaction piles (phase 2) and a test pile. The reaction piles in phase 1 were positioned at a spacing of 6 m (about 7.5 helix diameters from the tested pile). For phase 2, the reaction piles were positioned in a rectangular shape at distances of 4 and 3 m, so that a clear distance between any reaction pile and the test pile was about 6 helix diameters (2.5 m). Figure 3 shows the pile layout for phases 1 and 2. Four reaction piles were used to allow for the loading of piles to their ultimate load (failure load). Upon completion of the test program, all test and reaction piles were removed by reverse rotation.

Schematic sectional drawings of the load test arrangements and oblique views for the axial compression pile load tests for phases 1 and 2 are presented in Fig. 4, and for axial tension (uplift) load tests are presented in Fig. 5. For phase 1, the 150 ton (1 ton = 0.907 t) capacity test beam was centered over the test pile and supported on two reaction piles. The arrangements for applying loads to the test piles involved the use of an 800 kN hydraulic jack acting against

Table 1. Testing schedule and installation summary.

Pile No.	No. of helixes	Test type	Date	Installation torque (kN·m) (ft·lb in parentheses)	Embedment depth (m)
Phase 1 pile load testing					
C1	Single	Compression	9 July 2007	71.5 (52 700)	5.2
C2	Double	Compression	7 July 2007	88.1 (65 000)	5.0
T1	Single	Uplift	9 July 2007	72.5 (53 500)	5.1
T2	Double	Uplift	8 July 2007	84.7 (62 500)	5.1
L1	Single	Lateral	10 July 2007	71.9 (53 000)	5.2
L2	Double	Lateral	10 July 2007	86.8 (64 000)	5.2
Phase 2 pile load testing					
C3	Single	Compression	10 January 2008	52.3 (38 600)	5.3
C4	Double	Compression	9 January 2008	67.8 (50 000)	5.3
T3	Single	Uplift	12 January 2008	54.2 (40 000)	5.1
T4	Double	Uplift	11 January 2008	51.5 (38 000)	4.9
T5	Double	Uplift	12 January 2008	73.2 (54 000)	5.2

Table 2. Summary of boreholes and SPT results.

Soil layer	Depth of soil layer (m)	Penetration depth (m)	*N*-index (blows/ 300 mm penetration)
Location 1, phase 1			
Rock and sand	1.1	1.1	—
Oil sand	6.5*	2.5–2.8	64
		3.2–3.5	85
		4.5–4.8	Greater than 100
		6.2–6.5	26
Location 2, phase 2			
Rock and sand	2.2	0.9–1.2	11
		1.7–2.0	22
Oil sand	5.0*	2.5–2.8	67
		2.8–3.1	Greater than 100
		4.7–5.0	80

*Depth at the end of test hole.

Table 3. Summary of soil parameters.

			Friction angle, φ*	
Soil layer	Wet unit weight, γ (kN/m^3)	Dry unit weight, γ_{dry} (kN/m^3)	Peak	Residual
Compact sand	22.6	19.9	32	32
Oil sand	21.6	18.1	50	38

*Friction angle after Sharma et al. (1986).

the reaction beam. The test beam and reaction piles were tied with steel plates of 25 mm nominal thickness using 32 mm diameter all-thread Grade 8 steel bars. In axial compression tests, an additional steel bearing plate was placed between the top of the jack ram and the bottom of the test beam. Conversely, for the axial tension tests, the hydraulic jack was installed above the test beam and acted against a reaction frame that compressed an inverted pile cap and steel bearing plates. For phase 2, the 250 ton capacity test beam was centered over the test pile and supported on two reaction beams. Each of the two reaction beams were supported on two reaction piles. Load was applied using a 2500 kN hydraulic jack acting against the reaction beam.

The jacking system was equipped with a manually operated hydraulic pump and the jack pressure gauge readings were recorded manually. A visually read load cell was placed at the top of the test beam (centered at the test pile location) and connected to the test pile using a plate and tie rods. Pile head axial movements were monitored at two points during the test using independently supported dial gauges (0.025 mm accuracy, 50 mm travel). Another two dial gauges were used to monitor lateral movements. The dial gauges were connected to an independent reference beam and the tested pile. Another set of dial gauges (one dial gauge for each reaction pile) were installed to monitor the reaction pile movement at each load increment. An independent reference beam for pile movements was provided at each reaction pile location. The reference beam was supported at a minimum distance of 2.50 m from the test pile or reaction pile centers. Dial gauge readings were recorded manually at selected increments throughout the test duration.

Axial pile load tests were conducted according to the *Standard test method for piles under static axial compressive load*, ASTM D1143 (ASTM 1997*a*), and the *Standard test method for individual piles under static axial tensile*

Fig. 3. Pile load test layout for (*a*) phase 1 and (*b*) phase 2.

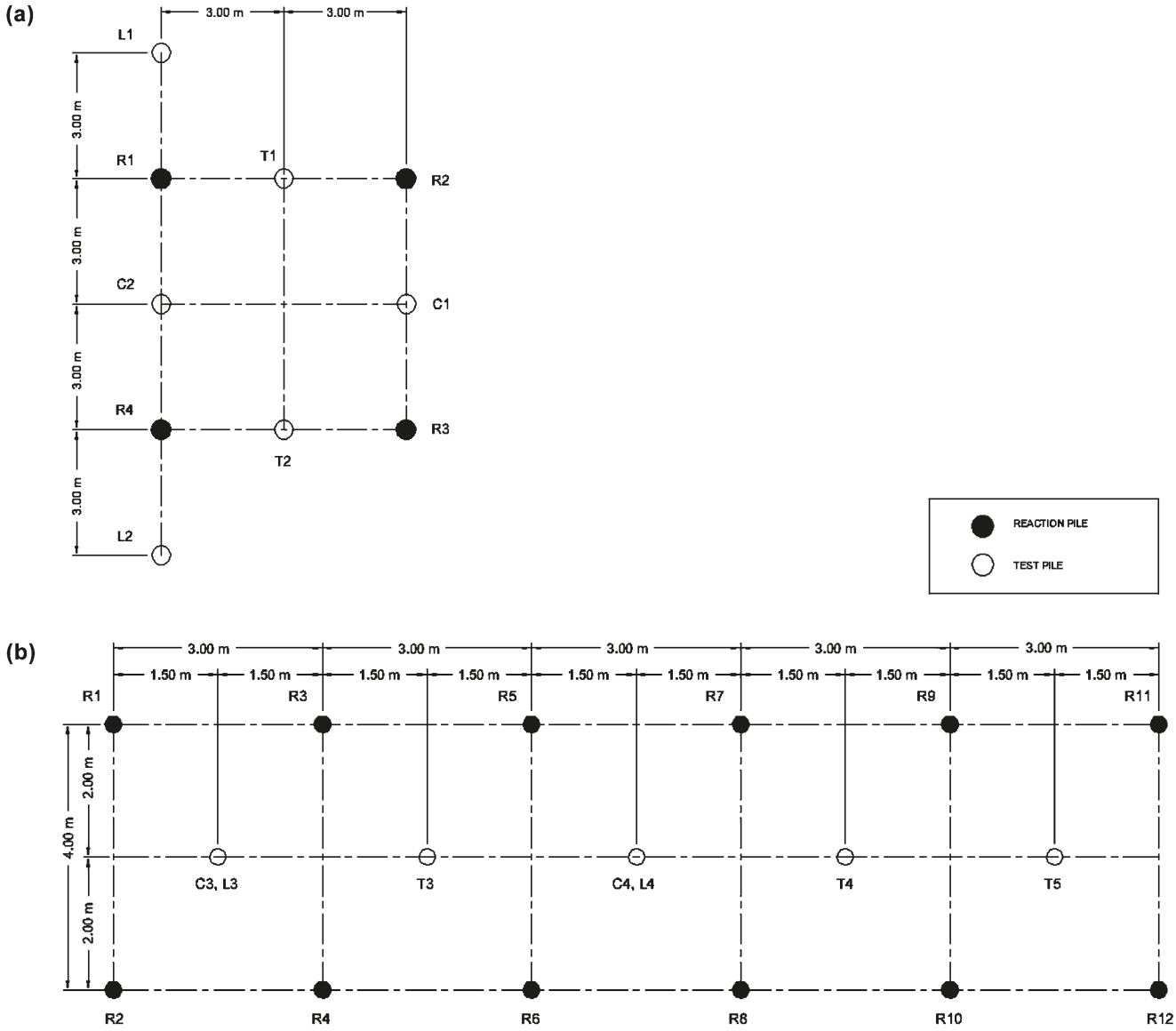

load, ASTM D3689 (ASTM 1997*b*). Loads were applied in increments of 10% of the estimated pile capacity in 10 min time intervals. In the first test series, loading was stopped at 800 kN due to the limitation of the hydraulic jack. However in the second testing series, loads were continued until continuous jacking was required to maintain the load (i.e., plunging failure — a failure where continuous pumping was required to maintain the load at the pile head).

Lateral load test setup

The lateral pile load test was conducted in general accordance with the *Standard test method for piles under lateral load*, ASTM D3966 (ASTM 1997*c*). A schematic sectional drawing of the lateral load test setup and an oblique view of the testing arrangements is shown in Fig. 6. The lateral load test setup consisted of a test pile that was installed at about 3 m away from a reaction pile. The reaction pile is typically a helical pile with a shaft diameter of 324 mm with double helixes 610 mm in diameter and was installed to a depth of about 5.2 m below ground surface. Loads were applied at a distance of about 300 mm above ground level using an 800 kN hydraulic jack. The hydraulic ram acted directly against a steel strut placed between the base of a hydraulic cylinder and the reaction pile.

The load testing system consisted of an 800 kN hydraulic jack and a hydraulic pump and pressure gauge with 69 MPa capacity. Lateral movements were monitored at two points along the pile free length (at distances of 50 and 300 mm above ground surface) to measure lateral deflections and rotation at the point of load application. The lateral deflections were measured using two independently supported micrometer dial gauges with 0.025 mm subdivisions and 50 mm travel. Lateral loads were applied in 2 kN increments in 10 min time intervals.

Test results

Axial compressive load test results

The results of axial compressive load tests are presented in Fig. 7 in the form of load–displacement curves for phases

Fig. 4. Axial compression load test setup: (*a*) schematic view; oblique view for test setup using (*b*) four reaction piles and (*c*) two reaction piles.

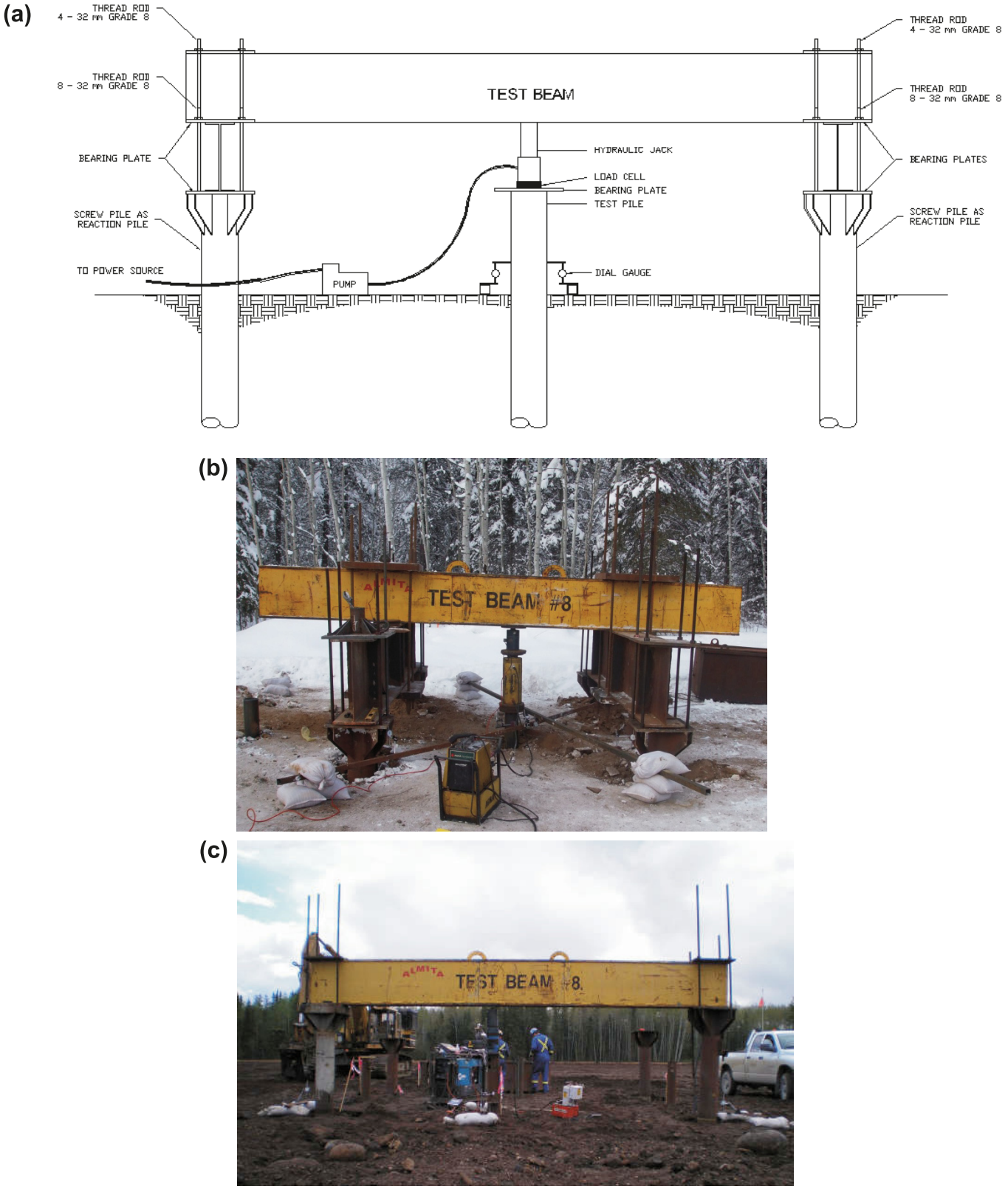

1 and 2. As indicated previously, the load tests in phase 1 (Fig. 7*a*) were terminated at axial loads of 800 kN due to equipment limitations. It can be seen from Fig. 7*a* that cycles were carried out at load of about 450 kN (for pile C1) and 180 kN (for pile C2) indicating that cyclic loading had a minor effect on the response.

Fig. 5. Axial tension (uplift) load test setup: (*a*) schematic view; oblique view for test setup using (*b*) four reaction piles and (*c*) two reaction piles.

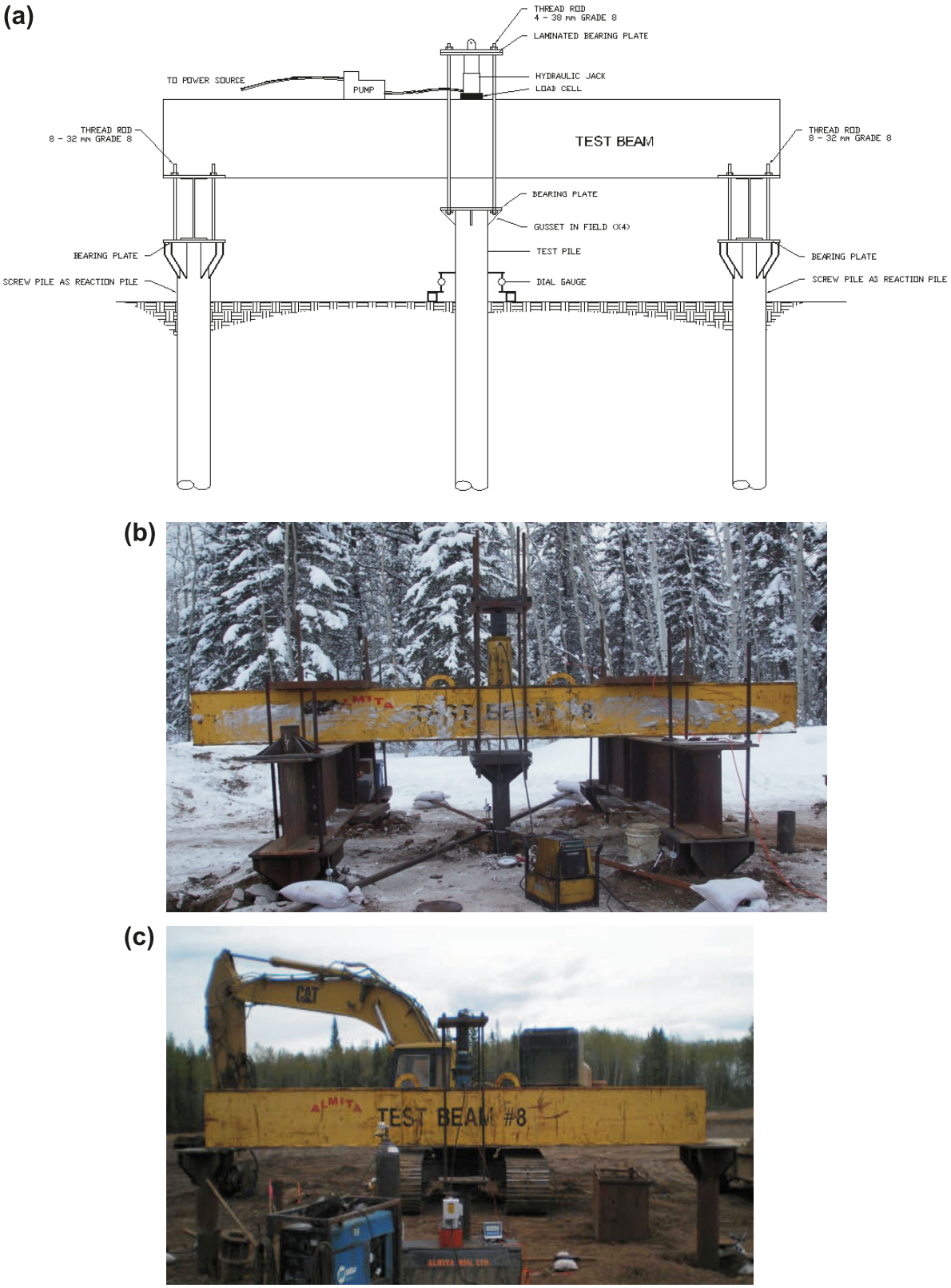

It can be seen from Fig. 7*b* that the load–displacement curves for tested piles include three different regions: a linear region with a steep slope (i.e., high stiffness), a transient nonlinear region with a gradually decreasing slope, and a final nearly linear region with a flat slope (i.e., low stiffness). Both piles C3 and C4 with single and double helixes showed

Fig. 6. Lateral load test setup: (*a*) schematic view and (*b*) oblique view for test setup.

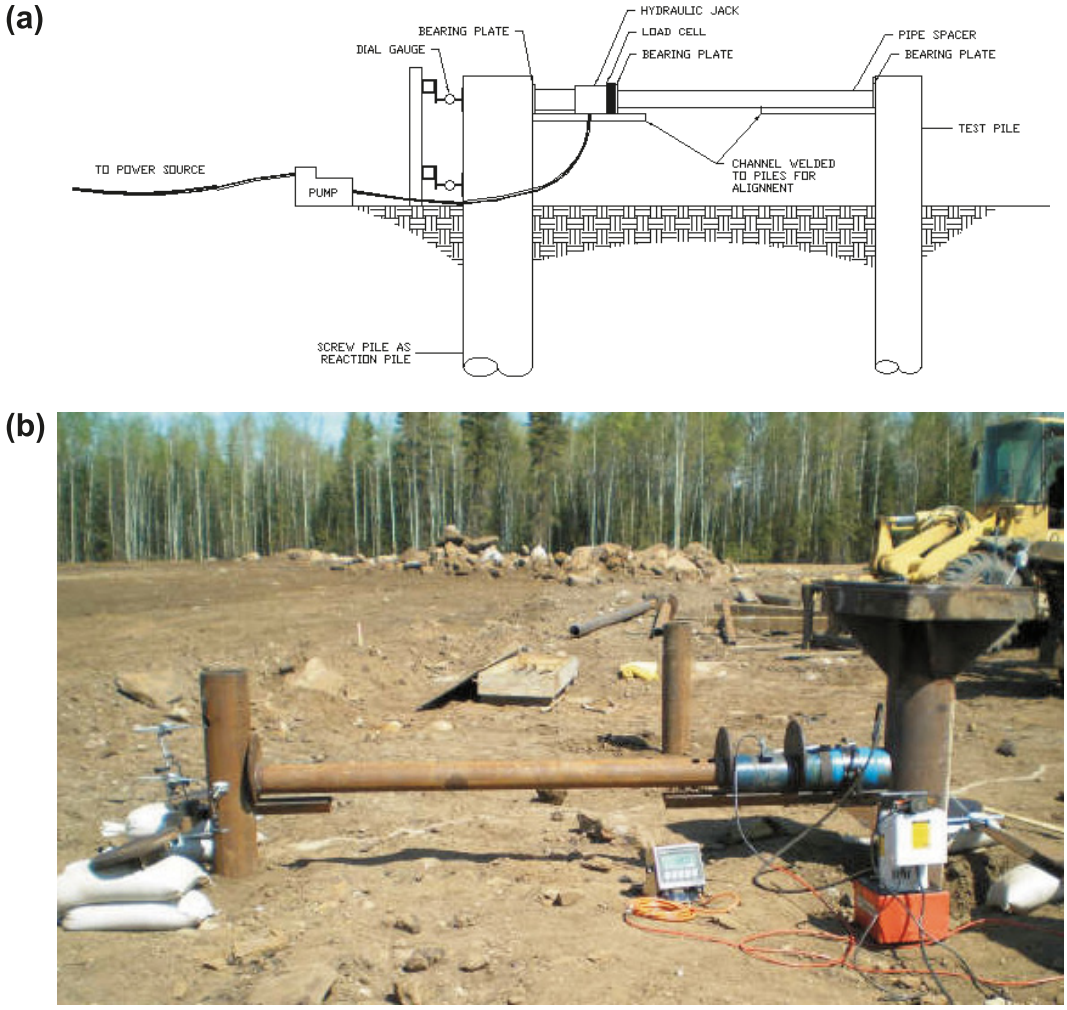

almost identical behavior at the early stages of loading up to loads of about 800 kN with corresponding displacements varying between 9 and 14 mm. However at higher settlement levels, pile C4 showed a stiffer response compared with pile C3. This response suggests that for pile C4 with double helixes, both helixes acted individually. The behaviour of pile C4 with double helixes and tested in cohesionless soil is in general agreement with the findings of Hoyt and Clemence (1989). Moreover, pile C3 showed plunging failure at a displacement of about 50 mm while pile C4 continued to resist loads up to the end of the test at a settlement of 40 mm.

Comparing piles C1 and C3 (see Figs. 7*a* and 7*b*) indicates that piles tested in phase 1 offered slightly stiffer response compared with piles tested in phase 2. This can be explained by the fact that oil sand for phase 1 of tests was present at a relatively shallow depth (depth of about 1.1 m) compared with 2 m for phase 2 (see Table 2 for soil properties).

It should be noted that the tested piles were recovered upon completing the tests by applying a reverse torque at pile heads and were visually inspected. There was no visible damage to the helixes, but pile shafts were polished as a result of significant friction during installation, testing, and removing the piles.

Axial compressive capacity

Terzaghi (1942) defined the axial compressive capacity of piles, Q_{uc}, as the load corresponding to a displacement equal to 10% of the pile diameter. This definition ensures that there is enough displacement to mobilize the end bearing component of the pile capacity. O'Neill and Reese (1999) defined the axial compressive capacity of cast-in-place concrete piles as the load that produces a movement at the pile head equal to 5% of the toe diameter. Livneh and El Nagger (2008) defined the ultimate compressive capacity of helical piles as the load associated with deflection equal to 8% of the diameter of the largest helix plus the elastic settlement of the pile. Similarly, the axial compressive capacity of helical piles can be defined as the load corresponding to a displacement level of 10% of the average helix diameter. This definition is suitable for helical piles as helix bearing capacity is a considerable component of the pile capacities. However, it should be noted that in many cases foundation design is controlled by the settlement tolerance, which is quite often less than 25 mm. Furthermore, the helix diameters may vary between 150 and 1219 mm. Hence, it may be more suitable to follow the O'Neill and Reese definition and to limit the maximum displacements by defining the axial capacities of helical piles

Fig. 7. Applied load at pile head versus settlement for axial compression pile load test for (*a*) phase 1 and (*b*) phase 2.

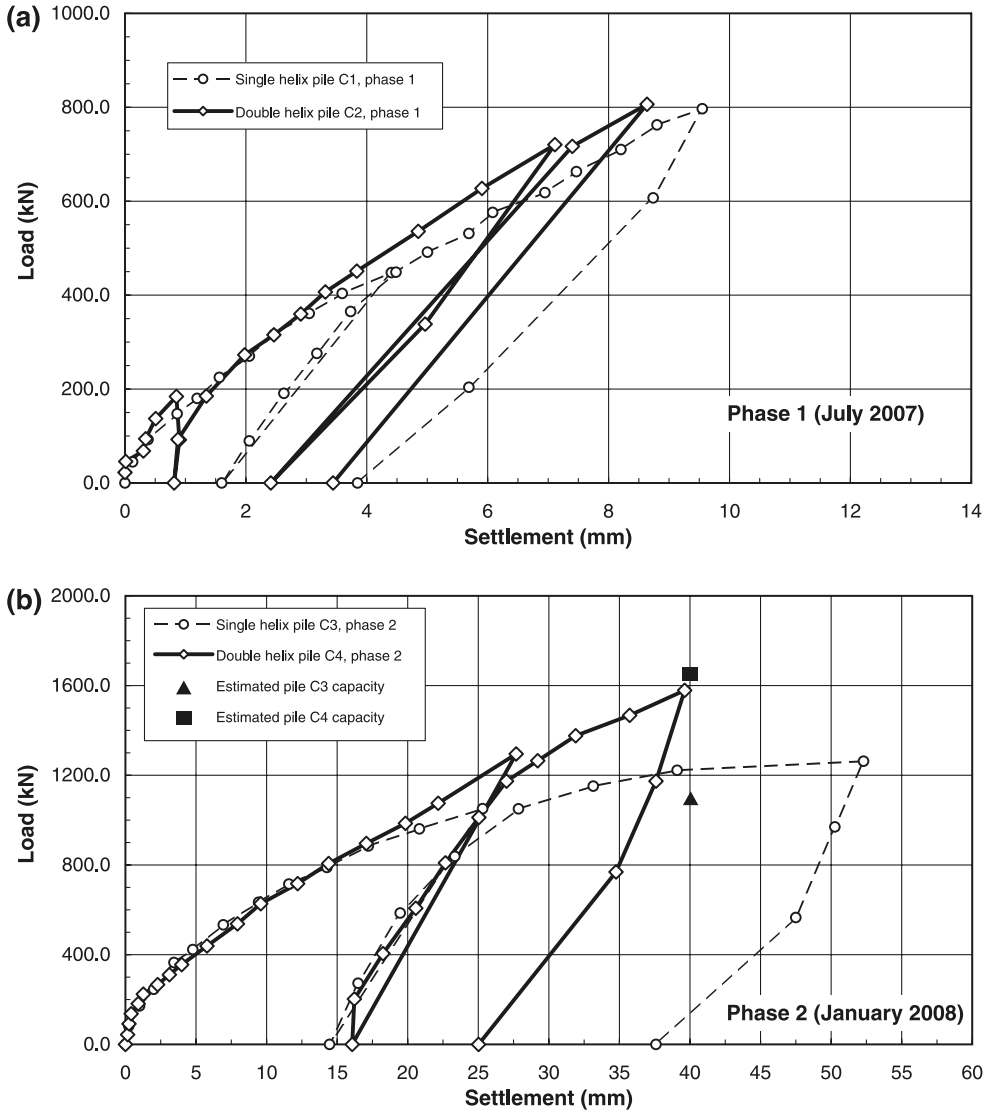

Table 4. Summary of axial compressive load test results.

		Measured ultimate pile capacity (kN)		Estimated ultimate pile capacity (kN)					
Pile No.	No. of helixes	10% of helix dia.	5% of helix dia.	Shaft resistance	Individual helixes	Ultimate pile capacity	Prediction ratio	Torque (kN·m)	K_T (m^{-1})
Compression test results									
C3	Single	1250	940	267	830	1097	0.88	52.3	23.9
C4	Double	1580	1000	267	1380	1647	1.04	67.8	23.3
Tension (uplift) test results									
T3	Single	620	560	258	307	565	1.01	54.2	10.3
T5	Double	960	820	258	576	834	1.02	73.2	11.2
T4	Double	720	630	177	439	616	0.98	51.5	12.2

based on the load applied at the pile head at a displacement level of 5% of average helix diameter.

The capacities for piles C3 and C4 are presented in Table 4. It can be seen from Table 4 that the capacities for piles C3 and C4 based on a 5% displacement criterion were 940 and 1000 kN, respectively, while the capacities based on a 10% failure criterion were 1250 and 1580 kN, respectively.

As suggested in the *Canadian foundation engineering manual* (Canadian Geotechnical Society 2006), the capacity of helical piles may be estimated from the following expression:

$$[1] \qquad R = \sum Q_h + Q_f$$

where R is the ultimate pile capacity, Q_h is the individual helix bearing capacity, and Q_f is the shaft resistance.

The individual helix bearing capacity can be estimated from the following expression:

$$[2] \qquad Q_h = A_h(S_u N_c + \gamma D_h N_q + 0.5\gamma D N_\gamma)$$

where A_h is the projected helix area, S_u is the undrained shear strength of the soil, γ is the unit weight of the soil, D_h is the depth to the helical bearing plate, D is the diameter of the helical plate, and N_c, N_q, and N_γ are bearing capacity factors for local shear conditions.

As indicated in the *Canadian foundation engineering manual* (Canadian Geotechnical Society 2006), the shaft resistance, Q_f, can be estimated from the following expression:

$$[3] \qquad Q_f = \sum \pi d \Delta L_i q_{si}$$

where d is the shaft diameter, ΔL_i is the pile segment length in soil layer i, and q_{si} is the average unit shaft friction of soil layer i

The unit shaft friction for the top compact sand layer can be estimated using $q_{si} = \sigma'_v K_s \tan(\delta)$, where σ'_v is the effective vertical stress at the mid-depth of each soil layer, K_s is the coefficient of lateral earth pressure ($K_s = 2(1 - \sin\varphi)$ for driven piles), and φ and δ are the frictional resistance and the interface friction angles, respectively.

Clementino et al. (2006) reported the results of full-scale pile load tests for cast-in place-concrete piles constructed in oil sand. Their test results indicated that the measured unit shaft friction for different piles varied between 250 and 410 kPa depending on the bitumen content. The lower unit shaft friction value corresponds to the lean oil sand (i.e., oil sand with bitumen content less than 6%) and the higher bound corresponds to rich oil sand (i.e., oil sand with bitumen content higher than 8%). These values are considerably higher than the unit shaft friction for very dense sands. The increased unit shaft friction for piles constructed in oil sand is due to the presence of bitumen within the voids. The estimated unit shaft friction for steel helical piles installed in lean oil sand considered in this study was 150 kPa assuming that the unit shaft friction for the oil sand–steel interface is 60% of the value for its oil sand–concrete interface.

The capacities of piles C3 and C4 are estimated using eqs. [1] through [3] and the results are presented in Table 4 as well. The estimated capacities were in reasonable agreement with the capacities based on a 10% failure criterion.

Axial tension (uplift) results

The results of axial tension (uplift) load tests presented in the form of load–displacement curves are plotted in Figs. 8*a* and 8*b* for phases 1 and 2. Similar to compression pile load test results, the initial parts of the load–displacement curves were linear up to a displacement level of about 3 mm, corresponding loads of about 440 kN (see Fig. 8*a*) and 320 kN (see Fig. 8*b*), followed by a nonlinear part. However at high displacement levels (i.e., greater than 10% of helix diameter as shown in Fig. 8*b*), both piles T3 and T4 with single and double helixes exhibited an asymptote (plateau). The asymptote for the piles gives the maximum resistance of the pile as described by Kulhawy and Hirany (1989). The stiffness of piles, which is defined as the slope of the load–displacement curve, was similar for piles T3 and T4 at the early stages of loading up to a displacement of about 3 mm. However at a higher displacement, pile T4 showed a stiffer response compared with pile T3, manifested as higher stiffness at the same displacement levels. Cycles were carried out at a load of about 450 kN for piles T1 and T2, indicating that the effect of cyclic loading had a minor effect on their response.

When comparing phases 1 and 2, piles T1 and T2 tested in phase 1 showed stiffer response compared with piles T3 and T4 tested in phase 2 due to the additional shaft frictional resistance gained from oil sand encountered at shallow depth for the test location in phase 1. Comparing between load–displacement curves for piles T3 and T4 with single and double helixes suggests that an additional uplift resistance of up to about 50% was gained for pile T4. This observation suggests that the individual helixes method is more suitable for estimating the uplift capacities of piles considered in the present study.

Effect of embedment depth into oil sand

To investigate the effect of embedment depth into the oil sand on the uplift behaviour of piles, an additional uplift load test (pile T5) was carried out at a location where the depth to the oil sand layer was about 3 m. The results are presented in Fig. 9, showing that the embedment depth into the oil sand has a major effect on the shaft resistance. The initial part of the load–displacement curve that presents the shaft friction was the steepest for the case of pile T2 (where depth to oil sand is 1.1 m) followed by pile T4 (depth to oil sand is 2 m) followed by pile T5 (depth to oil sand of 3 m). Therefore, the greater the pile embedment depth into the oil sand layer, the more shaft frictional resistance. The shaft resistance component for piles T2, T4, and T5 with a depth to oil sand of 1.1, 2, and 3 m was about 400, 320, and 250 kN, respectively. Moreover, for pile T4 the second part of the load–displacement, which represents the end bearing resistance, showed stiffer response compared with pile T5 due to the embedment depth into the oil sand and its role in increasing the end bearing pressure at the upper helix.

Uplift capacity

The uplift capacities of tested piles are also defined based on 10% and 5% failure criteria and the results are presented in Table 4. The capacities for piles T3 and T4 with single and double helixes based on 10% displacement criterion were 620 and 960 kN, respectively. The ultimate capacities of piles T3 and T4 at a displacement level of 5% were 560 and 820 kN, respectively. Comparing between the two failure criteria indicates that about 10% to 17% higher uplift capacities were obtained as a result of using a 10% failure criterion as opposed to a 5% failure criterion. Hence, defining the uplift capacity using a 5% failure criterion will provide a reasonable estimate of ultimate bearing capacity while maintaining reasonable displacement levels to satisfy serviceability requirements.

Fig. 8. Applied load at pile head versus displacement for axial tension (uplift) pile load test for (*a*) phase 1 and (*b*) phase 2.

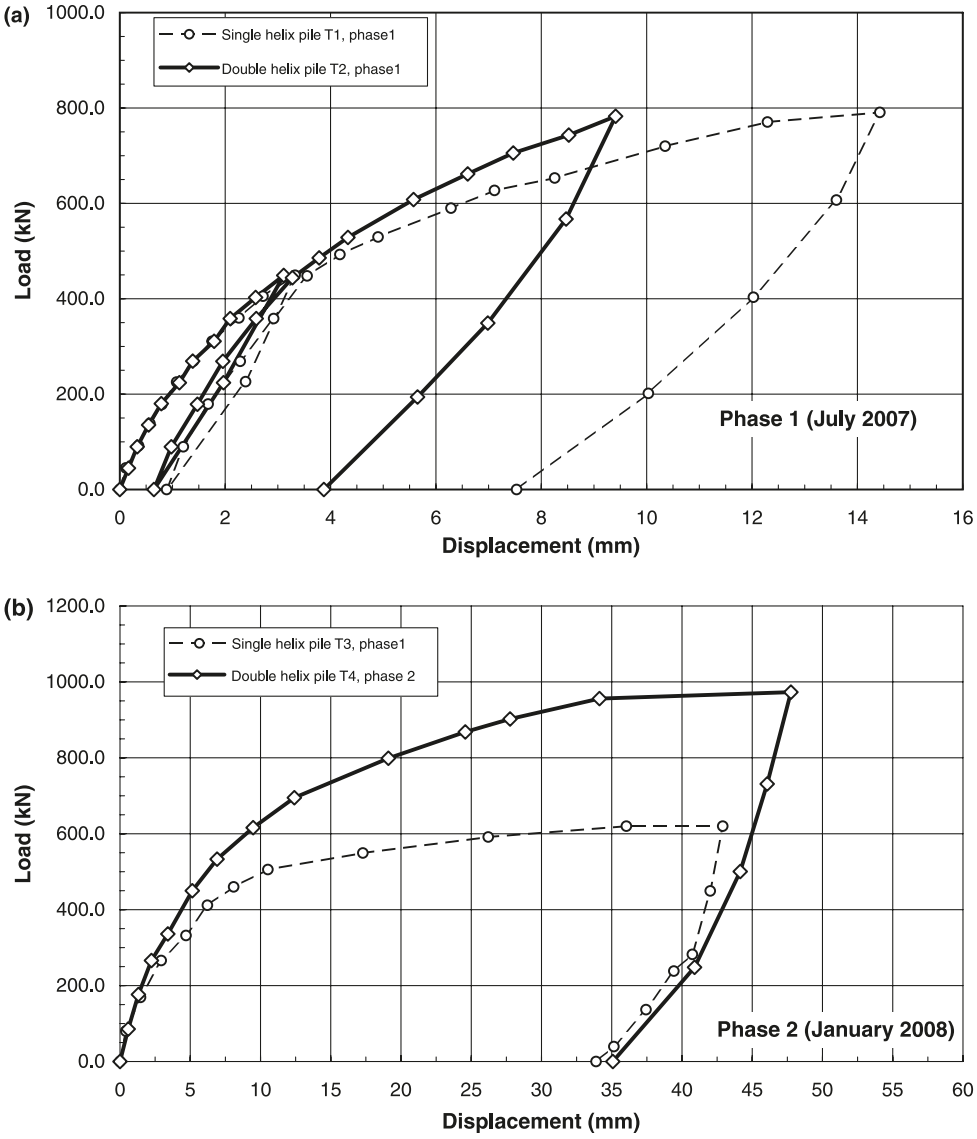

Similar to compressive loading, uplift capacity may be estimated using eq. [1] where the individual helix uplift capacity, Q_h, can estimated using eq. [4] (Das 1990) listed below.

$$[4] \qquad Q_h = A_h \gamma D_h F_q$$

where F_q is the breakout factor (Das 1990) defined as the ratio between the uplift bearing pressure and the effective vertical stress at the upper helix level. The following expression can be used to estimate the breakout factor (Das and Seeley 1975):

$$[5] \qquad F_q = 1 + 2\left[1 + m\left(\frac{D_{th}}{D_{uh}}\right)\right]\left(\frac{D_{th}}{D_{uh}}\right)K_U \tan\phi; \quad \text{where } (D_{th}/D_{uh}) \leq (D_{th}/D_{uh})_{cr}$$

where m is the coefficient dependent on soil friction angle, D_{th} is the embedment depth to the top helix; D_{uh} is the diameter of the upper helix, K_U is the nominal uplift coefficient, ϕ is the average frictional resistance angle for the soils above the upper helix, and $(D_{th}/D_{uh})_{cr}$ is the critical embedment ratio.

The breakout factor, F_q, depends on several parameters, such as the embedment depth ratio (D_{th}/D_{uh}), weight of soil above the top helix, shape of helix, and angles of internal friction for the soils above the upper helix. Merifield et al. (2006) concluded that the circular shape of the helixes provides higher resistance by about 20% compared with the square shape. It can be seen from eq. [5] that the F_q increase with embedment ratio until the critical embedment ratio, after which the F_q is independent of embedment depth. The estimated critical embedment ratio, $(D_{th}/D_{uh})_{cr}$, for the oil sand and compact sand layers above the upper helix considered in the present study was 6 and the corresponding critical embedment depth was 2.4 m. The estimated F_q values for the oil sand and compact sand layers were 40 and 20, respectively. The results of the estimated uplift capacities are also summarized in Table 4. The uplift capacities were estimated

Fig. 9. Effect of embedment depth into oil sand on the uplift capacity of helical piles.

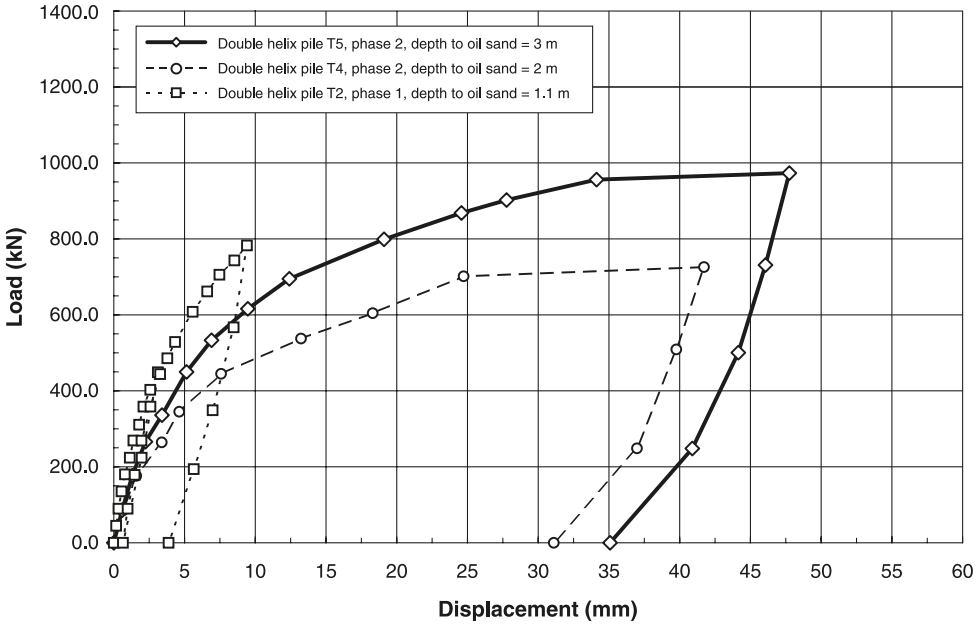

Fig. 10. Comparison between axial compression and uplift load test results.

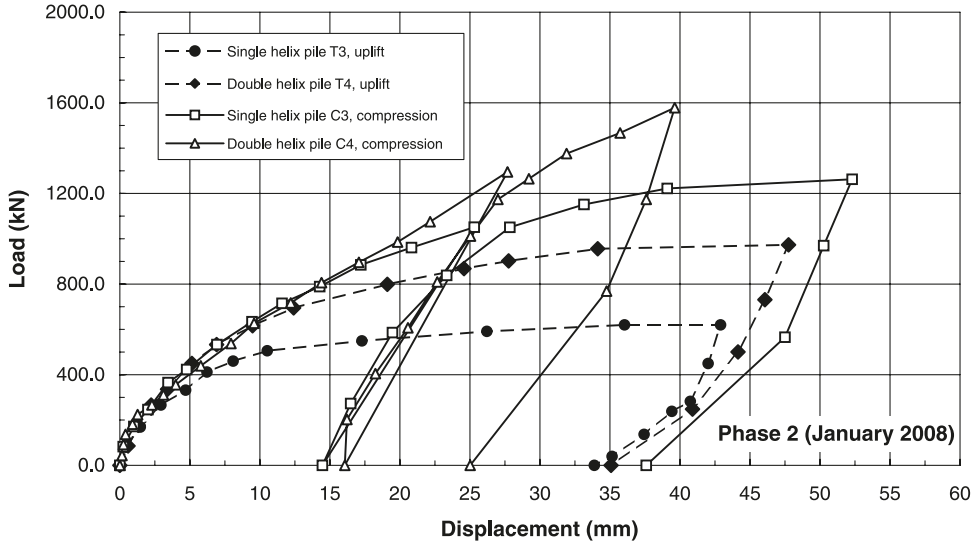

using eq. [1] and using soil parameters from Table 3. It should be noted that the 38° residual frictional resistance angle of oil sand was used. For pile T5 the frictional resistance angle was reduced to 36° to account for the proximity of the uppermost helix to the upper layer of compact sand. It can be seen from Table 4 that a reasonable agreement was obtained between measured and estimated uplift capacities.

Comparison between compressive and uplift load test results

The results of both compressive and uplift load tests for phase 2 are compared in Fig. 10. It can be seen from this figure that the load–displacement relationship was almost identical for all tests at the early stages of loadings up to a displacement of about 3 mm (about 0.75% of the helix diameter), which represented the pile shaft resistance. Therefore, the shaft friction for both compression and uplift loading was similar. However, at higher displacement levels, piles tested in compression offered higher resistance compared with piles tested in tension. Comparing between axial capacities of piles tested in compression and tension (Table 4) indicates that the compressive capacities of piles C3 and C4 were 40% to 50% higher than the uplift capacities of piles T3 and T4. The lower end-bearing resistance of helical piles tested in tension is due to the smaller projected area of the top helix compared with the total area of the bottom helix for piles tested in compression. In addition, soil conditions near the top and bottom helixes were different due to soil stratification and soil variability. Trofimenkov and Mariupolskii (1965) conducted a series of field compression and tension tests using screw piles with various soil types. About 200 piles were installed in soft to hard clays as well as loose to medium-dense sands with pile helix diameter D ranging from 0.45 to 1.0 m to a depth up to 7 m.

The test results indicated that the compression capacity was 1.4 to 1.5 times higher than the uplift capacity. These results were in general agreement with helical piles tested in oil sand in the present study.

Another comparison between piles tested in compression and tension can be made using the stiffness at the pile head, defined as the slope of the load–settlement curves. In general, the pile stiffness in compression load tests was larger than those of piles tested in tension. The rate of reduction of stiffness at high displacement levels for piles tested in compression was higher than those piles tested in tension.

Installation torque – pile capacity relationship

Despite the lack of geotechnical explanation, empirical methods have been established for a relation between torque and ultimate pile capacity. It has been statistically analyzed based on a large database, and the method has been used successfully in the construction of thousands of anchors over the past 20 years as indicated by Hoyt et al. (1995). The empirical relationship can be expressed as (Hoyt and Clemence 1989; Canadian Geotechnical Society 2006)

$$[6] \qquad Q_t = K_t T$$

where K_t is an empirical factor and T is the average installation torque.

The torque–load correlation factor, K_t, for compression and uplift loading found in this study are presented in Table 4. It can be seen from Table 4 that the ratios of torque to compressive capacity for piles with single and double helixes were 23.9 m^{-1} (7.3 ft^{-1}) and 23.3 m^{-1} (7.1 ft^{-1}), respectively. The values of K_t for tension piles varied between 10.3 m^{-1} (3.1 ft^{-1}) for piles with a single helix and 11.2 m^{-1} (3.4 ft^{-1}) and 12.2 m^{-1} (3.7 ft^{-1}) for piles with double helixes. Although these values are in agreement with the findings reported in the literature (Hoyt and Clemence 1989; Canadian Geotechnical Society 2006), it should be noted that torque–load correlations reported in the literature are established for small diameter anchors resisting uplift loads. Therefore, those correlations should be used with caution to estimate the uplift capacities of large diameter helical piles due to the size effect and shape of the shaft (i.e., square or round shaft). However, torque–load correlations cannot be used to estimate the axial compressive capacities of helical piles due to the differences in the compression and uplift failure mechanisms and variability of soils near the top and bottom helixes. Moreover, the torque exerted during pile installation is dependent on several factors, such as the operator experience, vertical forces exerted on the pile during installation, helix shape, pitch size, and frequency of calibrating the equipment. In addition, for the case of helical piles installed to resist compression loads, torque reported during installation cannot predict the strength of the soil layer immediately below the lower helix that will considerably impact the compressive strength of helical piles. For the above-mentioned reasons, it is the author's opinion that torque–load correlations may be used as quality assurance, but not for design purposes.

Lateral load test results

The horizontal deflection near the pile head y_o, (at about 300 mm above ground) versus the applied load at the pile head for pile L1 with a single helix and pile L2 with double helixes are plotted in Fig. 11. It can be seen from Fig. 11 that the lateral responses of both piles were nonlinear. Piles L1 and L2 were loaded to maximum loads of about 43 and 42 kN, respectively, which corresponded to maximum deflections of about 35 and 38 mm. When piles rebounded to zero load, the net or permanent displacement was about 7 mm and 5 mm for piles L1 and L2, respectively.

A comparison between the responses of piles L1 and L2 indicates that pile L1 with a single helix showed slightly higher resistance compared with pile L2 with double helixes. This observation suggests that the lateral resistance of helical piles is independent of the helix configuration and is governed mainly by the shaft diameter. Therefore, the role of helixes in providing additional lateral resistance is minor given that the helixes are relatively deep (i.e., considered as long piles). Slight variations in the lateral resistance of piles L1 and L2 may be due to disturbance of the soil during helical pile installation. Similar observations were reported by Puri et al. (1984) during their small-model testing using screw anchors.

Gaps were formed behind the piles during testing, indicative of plastic deformation of the soil in front of the pile. Upon examination of each of the piles after the test, no significant bending deformation of the shafts or other visible pile damage were noted, as would be indicative of pile structural failure or the development of a plastic hinge during the test. Figure 11*b* show that the rotation at the ground surface, θ_o, for pile L1 was less than that of pile L2 at all loading stages. Rotation for both piles increased with the increase in lateral load, which is consistent for a free head pile condition.

Lateral capacity of tested piles

The ultimate lateral load of piles is usually specified to satisfy a limiting lateral deflection criterion. This may result in specifying an "ultimate" lateral load that is much lower than the ultimate lateral capacity of the pile. For the helical piles with relatively short lengths considered in the present study, failure usually occurs by rotation of the pile within the soil. In this case, a large displacement is required to mobilize the passive resistance of the soil near the pile head and at the pile toe. Therefore, in the absence of a distinct failure criterion, and as the design of laterally loaded piles is generally governed by the lateral deflection of the superstructure, the ultimate lateral load is defined as the load that corresponds to a lateral deflection of 6.25 mm as suggested by Prakash and Sharma (1990). It should be also noted that a lateral deflection in the order of 12.5 mm is often considered for the design of foundation supporting structures that are less sensitive to lateral movements, such as power transmission lines.

The ultimate lateral load capacity, Q_l, is established based on the above criteria and the values for all piles are presented in Table 5. Table 5 shows that the lateral resistance of pile L1 with a single helix was similar to that of pile L2 with double helixes at a low deflection level of about 6.25 mm. However at a relatively higher deflection levels (i.e., deflection level of 12.5 mm), pile L2 showed a slightly lower resistance than pile L1.

Fig. 11. Lateral load test results: (*a*) load–deflection and (*b*) load–rotation curves.

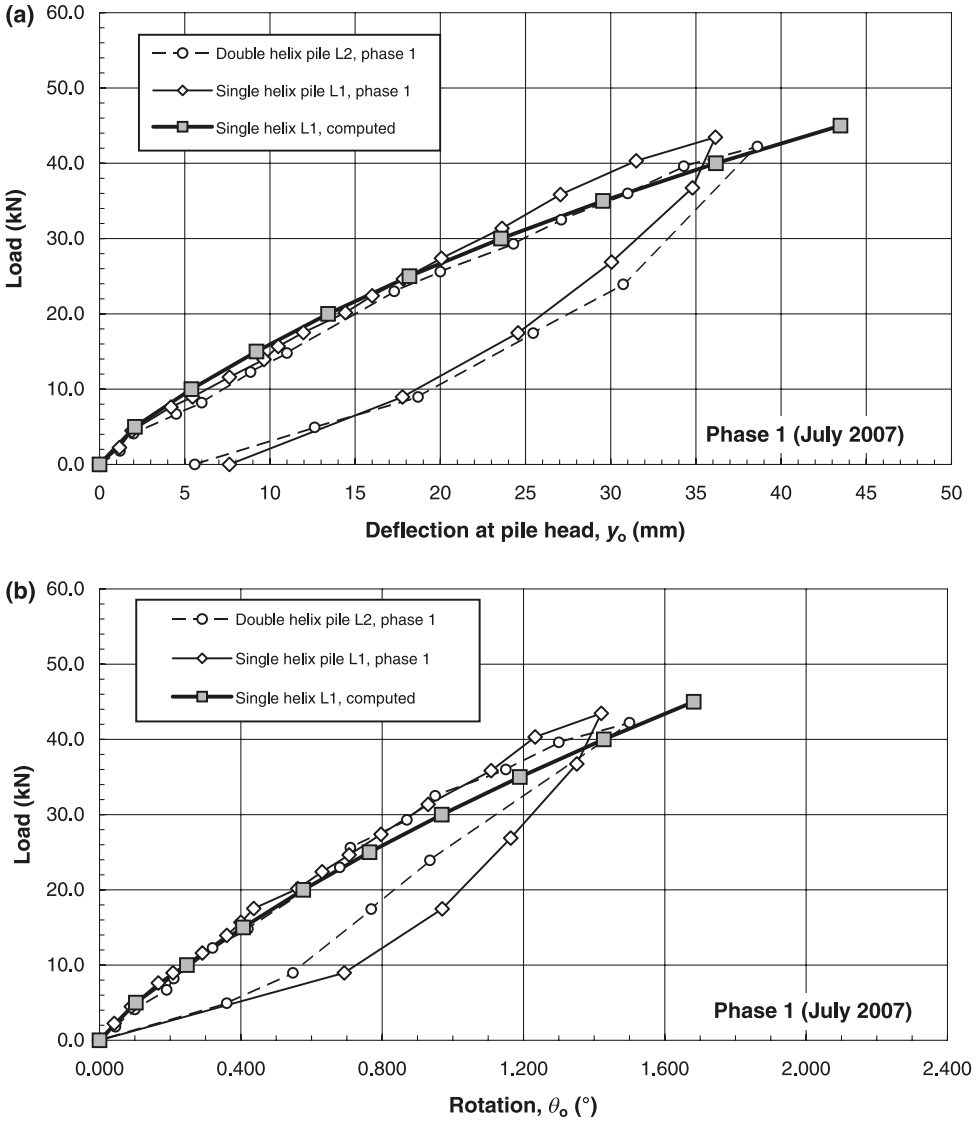

Table 5. Lateral load test results.

Pile No.	Pile type	Pile lateral resistance, Q_l, at 6.25 mm deflection (kN)	Pile lateral resistance, Q_l, at 12.5 mm deflection (kN)	Lateral resistance at end of test (kN)	Lateral deflection at end of test (mm)
L1	Single helix	10	18	43	35
L2	Double helix	9	16	42	38

Comparison between measured and estimated lateral resistance of helical piles

The computer program LPILE Plus (Ensoft Inc. 2005), based on the *p*–*y* curves developed by Reese et al. (1974), is widely used to predict the response of laterally loaded piles. Soil parameters used in the analyses are provided in Table 3. It has been assumed that soil layers consisted of compact sand extending from the ground surface to a depth of 1.1 m below ground over very dense oil sand extending to the bottom of the piles. Analyses were carried out for both piles L1 and L2 with a free head condition. The results of the load–deflection relationship and rotation versus load at the pile head were compared with measured values (see Fig. 11). It can be seen from Fig. 11 that both measured and estimated values agreed reasonably. Figure 11 also suggests that interaction between the shaft and soil is the most significant when resisting the lateral loads and the soil between the helixes played a minor role in the lateral resistance.

Conclusions

A full-scale pile load testing program was carried out using single- and double-helix piles to investigate their performance under axial compressive, uplift, and lateral loading conditions. The findings of this study can be summarized in the following conclusions:

(1) Helical piles with a relatively small shaft and helix sizes were successfully installed into oil sand soil and resisted high compression and tension loads.
(2) The load–displacement curves of piles tested in compression displayed typical trends including an initial linear segment followed by a highly nonlinear segment and a near-linear segment. Helical piles with double helixes provided about 40% higher resistance compared with piles with a single helix. Therefore, the use of an additional helix, which adds only a minimal cost, is a very cost-effective method for increasing the capacity of helical piles.
(3) A comparison between load–settlement curves for single- and double-helix piles with a spacing ratio, S/D, of 3 suggested that the developed load failure mechanism was through the individual helixes. Therefore, the use of the individual helix method is more suitable for estimating the axial capacities of helical piles (with $S/D = 3$) embedded into oil sand.
(4) The load–displacement curves for piles subjected to uplift loads indicate that a typical trend consisted of an initial linear segment followed by a nonlinear segment followed by an asymptote (plateau).
(5) A failure criterion was proposed to estimate the ultimate uplift capacities of helical piles at a displacement level of 5% of the average helix diameter.
(6) A comparison between the compression and uplift load tests suggested that similar magnitude shaft resistance was developed for both compression and uplift load tests. However, the end bearing component of uplift capacity of the helical piles was controlled by the soils above the top helix.
(7) A correlation between torque and axial capacity of piles may exist. However, it should be recognized that the torque factors for both axial compression and uplift load conditions are different due to the differences in both failure mechanisms and variation in soil stratifications at the upper and lower helixes. Moreover, full-scale static load tests are considered the most accurate method for estimating helical pile capacities. Therefore, it is recommended to carry out a full-scale static load test for relatively large projects to validate the axial capacities of the design piles and to evaluate the torque factors that can be used to correlate between torque and pile capacity of the production piles. Then the torque–pile capacity relationship may be used throughout the project site for quality assurance purposes.
(8) The results of lateral load tests carried out in this study confirmed that helical piles can develop significant resistance to lateral loads.
(9) The lateral load versus deflection behaviour of a helical pile is controlled mostly by the size of the shaft (i.e., diameter and thickness). The helixes had a minor effect on the lateral behavior of helical piles.
(10) The use of multiple helixes may slightly reduce the lateral resistance of piles due to additional soil disturbance. However, further investigation is required to confirm this hypothesis.
(11) The lateral load resistance may be estimated analytically using a p–y curves approach. A comparison between measured and estimated lateral resistance of helical piles using the LPILE Plus 5 program indicated that a reasonable agreement was obtained.

Acknowledgements

The author would like to extend his gratitude to his employer and ATCO Structures for the opportunity to carry out the load testing program at their site. The author would like to thank his co-workers and field staff for their patience, attention to details, and careful installation and load testing methods for piles considered in this study. In particular, the author would like to thank Larry Kaumeyer, Richard Schmidt, Colin McCann, and Patrick Lentz.

References

ASTM. 1997*a*. Standard test method for piles under static axial compressive load. ASTM standard D1143–81 (reapproved 1994). *In* Annual book of ASTM standards. ASTM International, West Conshohocken, Pa. Vol. 04.08. pp. 95–105.

ASTM. 1997*b*. Standard test method for individual piles under static axial tensile load. ASTM standard D3689–90 (reapproved 1995). *In* Annual book of ASTM standards. ASTM International, West Conshohocken, Pa. Vol. 04.08. pp. 366–375.

ASTM. 1997*c*. Standard test method for piles under lateral load. ASTM standard D3966–90 (reapproved 1995). ASTM International, West Conshohocken, Pa.

Canadian Geotechnical Society. 2006. Canadian foundation engineering manual. 4th ed. BiTech Publishers Ltd., Richmond, B.C.

Clementino, R., Tweedie, R., Sobkowicz, J., Workman, C., and Sisson, R. 2006. High capacity cast-in-place concrete pile load tests at cnrl's oil sand plant near Fort McMurray, Alberta. *In* Proceedings of the 59th Canadian Geotechnical Conference, Vancouver, B.C., 1–4 October 2006. Canadian Geotechnical Society, Richmond, B.C. pp 57- 64.

Das, B.M. 1990. Earth anchors. Elsevier, Amsterdam, the Netherlands.

Das, B.M., and Seeley, G.R. 1975. Breakout resistance of horizontal anchors. Journal of the Geotechnical Engineering Division, **101**(9): 999–1003.

Ensoft Inc. 2005. LPILE PLUS 5: A program for the analysis of piles and drilled shafts under lateral loads. Version 5.0.39 [computer program]. Ensoft Inc., Austin, Tex.

Hoyt, R.M., and Clemence, S.P. 1989. Uplift capacity of helical anchors in soil. *In* Proceedings of the 12th International Conference on Soil Mechanics and Foundation Engineering, Rio de Janeiro, Brazil, 13–18 August 1989. Balkema, Rotterdam, the Netherlands. Vol. 2. pp. 1019–1022.

Hoyt, R., Seider, G., Reese, L.C., and Wang, S.T. 1995. Buckling of helical anchors used for underpinning. *In* Foundation Upgrading and Repair for Infrastructure Improvement, Proceedings of the Symposium held in conjunction with the ASCE Convention, San Diego, Calif., 23–26 October 1995. *Edited by* F.K. William and J.M. Thaney. Geotechnical Special Publication No. 50. American Society of Civil Engineers (ASCE), New York. pp. 89–108.

Kulhawy, F.H., and Hirany, A. 1989. Interpretation of load tests on drilled shafts — Part 2: Axial uplift. *In* Foundation Engineering: Current Principles and Practices, Proceedings of the ASCE Foundation Engineering Conference, Evanston, Ill., 25–29 June 1989. *Edited by* F.H. Kulhawy. American Society of Civil Engineers (ASCE), New York. Vol. 2. pp. 1150–1159.

Lade, P.V., and Duncan, J.M. 1975. Elasto-plastic stress strain theory for cohesionless soil. Journal of the Soil Mechanics and Foundations Division, ASCE, **101**(10): 1037–1053.

Livneh, B., and El Nagger, M.H. 2008. Axial testing and numerical modeling of square shaft helical piles under compressive and tensile loading. Canadian Geotechnical Journal, **45**(8): 1142–1155. doi:10.1139/T08-044.

Merifield, R.S., Lyamin, A.V., and Sloan, S.W. 2006. Three-dimensional lower bound solutions for the stability of plate anchors in sand. Géotechnique, **56**(2): 123–132. doi:10.1680/geot.2006.56.2.123.

Meyerhof, G.G., and Adams, J.I. 1968. The Ultimate uplift capacity of foundations. Canadian Geotechnical Journal, **5**(4): 225–244. doi:10.1139/t68-024.

Mitsch, M.P., and Clemence, S.P. 1985. The uplift capacity of helix anchors in sand. *In* Proceedings of Uplift Behavior of Anchor Foundations in Soil, Detroit, Mich., 24 October 1985. *Edited by* S.P. Clemence. American Society of Civil Engineers (ASCE), New York. pp. 26–47.

Narasimha Rao, S., Prasad, Y.V.S.N., and Shetty, M.D. 1991. The behaviour of model screw piles in cohesive soils.. Journal of Soil and Foundations, **31**: 35–50.

O'Neill, M.W., and Reese, L.C. 1999. Drilled shafts: Construction procedures and design methods. Office of Infrastructure, Federal Highway Administration, Washington, D.C. Publication No. FHWA-IF-99–025.

Prakash, S., and Sharma, H.D. 1990. Pile foundations in engineering practice. John Wiley and Sons, New York.

Puri, V.K., Stephenson, R.W., and Goen, L. 1984. Helical anchor piles under lateral loading. *In* Laterally loaded deep foundations: Analysis and performance. ASTM STP 835. *Edited by* J.A. Langer, E.T. Mosley, and C.D. Thompson. American Society for Testing and Materials, West Conshohocken, Pa. pp. 194–213.

Reese, L.C., Cox, W.R., and Koop, F.D. 1974. Analysis of laterally loaded piles in sand. *In* Proceedings of the 5th Annual Offshore Technology Conference, Houston, Tex., 6–8 May 1974. Offshore Technology Conference, Richardson, Tex. Paper OTC 2080. pp. 473–483.

Sakai, T., and Tanaka, T. 1998. Scale effects of a shallow circular anchor in dense sand. Soils and Foundations, **38**(2): 93–99.

Scott, J.D., and Kosar, K.M. 1984. Geotechnical properties of Athabasca oil sands. *In* Proceedings of the WRI-DOE Tar Sand Symposium, sponsored by Western Research Institute and U.S. Department of Energy, Vail, Colo., 26–29 June 1984. pp. 1–32.

Sharma, H.D., and Joshi, R.C. 1988. Drilled pile behaviour in granular deposits. Canadian Geotechnical Journal, **25**: 222–232. doi:10.1139/t88-026.

Sharma, H.D., Haris, M.C., Scott, J.D., and McAllister, K.W. 1986. Bearing capacity of bored cast-in-place concrete piles on oil sand. Journal of the Geotechnical Engineering Division, **112**(12): 1101–1116. doi:10.1061/(ASCE)0733-9410(1986)112:12(1101).

Tagaya, K., Tanaka, A., and Aboshi, H. 1983. Application of finite element method to pullout resistance of buried anchor. Soils and Foundations, **23**(3): 91–104.

Tagaya, K., Scott, R.F., and Aboshi, H. 1988. Pullout resistance of buried anchor in sand. Soils and Foundations, **28**(3): 114–130.

Terzaghi, K. 1942. Discussion of the progress report of the committee on the bearing value of pile foundations. Proceedings of the American Society of Civil Engineers, **68**: 311–323.

Trofimenkov, J.G., and Mariupolskii, L.G. 1965. Screw piles used for mast and tower foundations. *In* Proceedings of the Sixth International Conference on Soil Mechanics and Foundation Engineering, Montréal, Que., 8–15 September 1965. University of Toronto Press, Toronto, Ont. Vol. 11. pp. 328–332.

Vesic, A.S. 1971. Breakout resistance of objects embedded in ocean bottom. Journal of the Soil Mechanics and Foundations Division, ASCE, **97**(SM9): 1183–1205.

Zhang, D.J.W. 1999. Predicting capacity of helical screw piles in Alberta soils. M.Sc. thesis, University of Alberta, Edmonton, Alta.